Supporting Information

Experimental Section:

Synthesis of PdPS: The ternary phosphochalcogenide with formula, PdPS was prepared by a modified high temperature solid state synthesis, from pure elements in evacuated, sealed quartz tube, based on a reported procedure (reference 20 from the main manuscript). The constituent lements (Pd,P,S) in the molar ratio 1:1:1 were thoroughly mixed in presence of a volatile solvent (isopropanol) and the resulting dry mixture was transferred to a quartz tube, either as powder or as a pellet. The quartz tube was sealed after evacuating through a vacuum line (~10^{-6} mbar). Subsequently, the sealed tube was kept at 950°C for seven days and slowly cooled to 25ºC. The product was removed by breaking the tube under ambient conditions. The shiny silvery crystals were separated and subsequently used for further studies.

Synthesis of rGO-PdPS nanocomposite: Large and few-layer graphene oxide nanosheets were prepared by modified Hummers' method as reported earlier (reference 24). The rGO-PdPS composite was prepared by mixing 20 mg of PdPS with 20 mL of 1 mg mL^{-1} aqueous graphene oxide colloid. The colloid was sonicated for 30 minutes, transferred to a teflon lined autoclave and kept at 180°C for 20 hours that led to a stable dispersion. It was washed with water with resistivity 18 MΩcm obtained from milli-Q system and dried in vacuum at 80°C to obtain in-situ reduced graphene oxide - PdPS composite denoted as rGO-PdPS.

Preparation of catalyst modified electrode: The HER activity was studied at 25°C in an electrochemical cell containing three electrodes with 0.5 M H_2SO_4 (pH 0.8) as the electrolyte, saturated calomel electrode (SCE) and Pt foil as reference and counter electrodes respectively. The catalyst layer was fabricated as follows: 10 mg of the catalyst (rGO-PdPS composite) was mixed with 2 mL of isopropanol by stirring for 30 minutes and subsequently, 20 μL of nafion (perfluorosulphonic acid based resin provided as 5% solution in lower aliphatic alcohols, Aldrich, USA) solution was added to obtain a stable slurry. An amount of 10 μL of the slurry was spread on a glassy carbon disk surface of area 0.07 cm^2 and dried under ambient conditions. The loading of catalyst was in the range of 1 - 2 mg cm^{-2}.

Characterization:

The morphology of PdPS and its composite with rGO were characterized by scanning electron microscopy (SEM) using Carl Zeiss ultra 55 SEM equipped with energy dispersive X-ray analysis accessory (EDAX). The operating voltage was between 5 and 10 kV. Transmission electron microscopy (TEM), HRTEM, elemental mapping and selected area electron diffraction (SAED) were obtained using JEOL 2200F TEM operated at 200 kV. The samples for TEM analyses were prepared by sonicating the catalyst in isopropanol, followed by drop casting on carbon - coated copper grids and subsequent drying. The SEM samples were prepared by drop coating the dispersion on highly doped Si surface. X-ray diffraction (XRD) patterns were recorded using Philips diffractometer (PANanlytical with Cu-Kα radiation, λ= 1.5406 Å). X-ray photoelectron spectroscopic (XPS) measurements were performed using Axis ultra (Multi technique X-ray photoelectron spectroscopy, UK) spectrometer with Al Kα (1486.6 eV) as the source. The data analysis was carried out using XPSpeakfit 4.1 software. Electrochemical measurements were carried out using CH660A (USA) electrochemical system in a three-electrode cell. Electrode potentials were recorded vs SCE reference electrode, and subsequently calibrated[25] with respect to RHE. All the potentials are referred to RHE according to the relation, E (RHE) = E (SCE) + 0.259 V based on the calibration (Supporting Information, Figure S12) plot as described in the supporting information. Galvanostatic electrolysis was performed in a divided H- shaped cell and the evolved hydrogen gas was collected by inversion burette method.

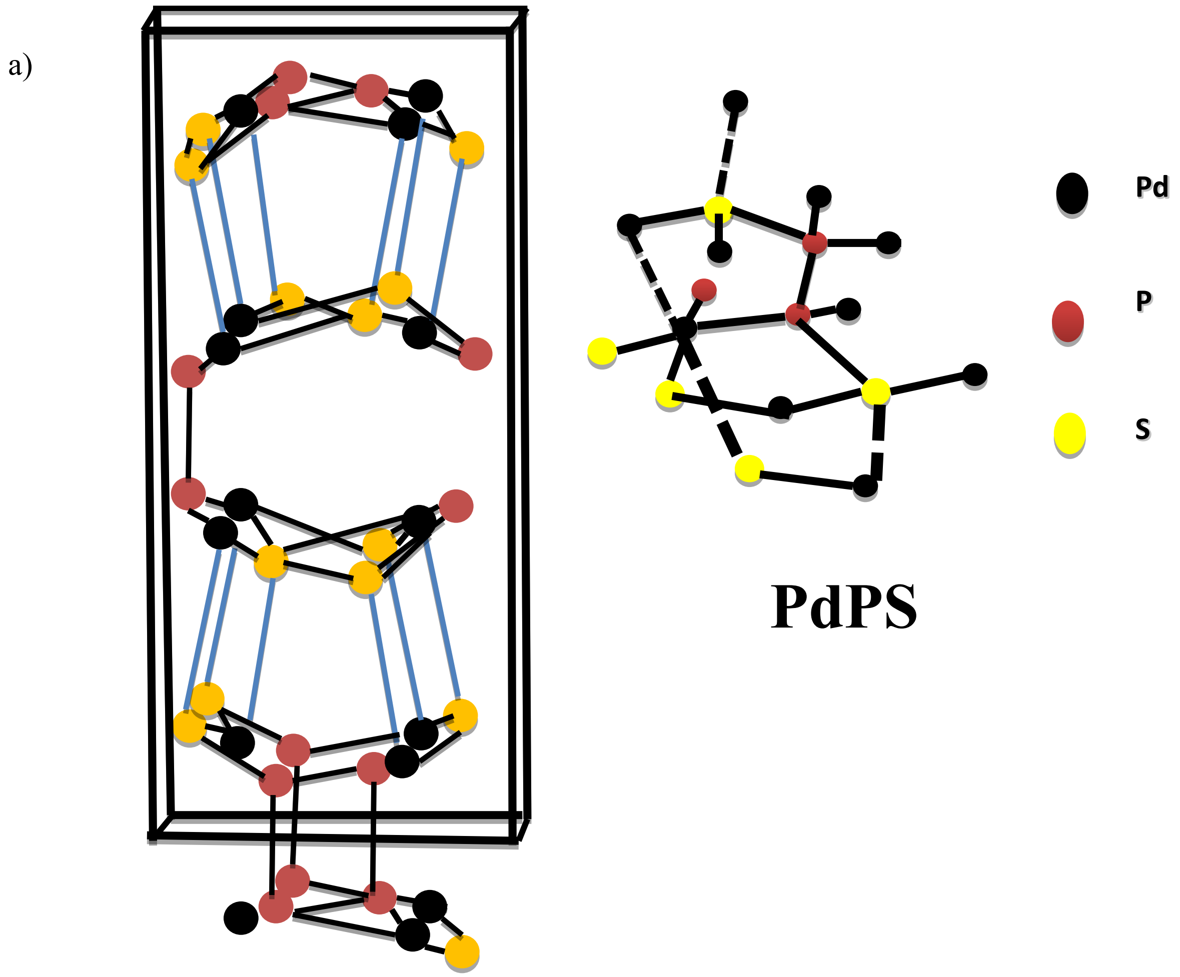

b)

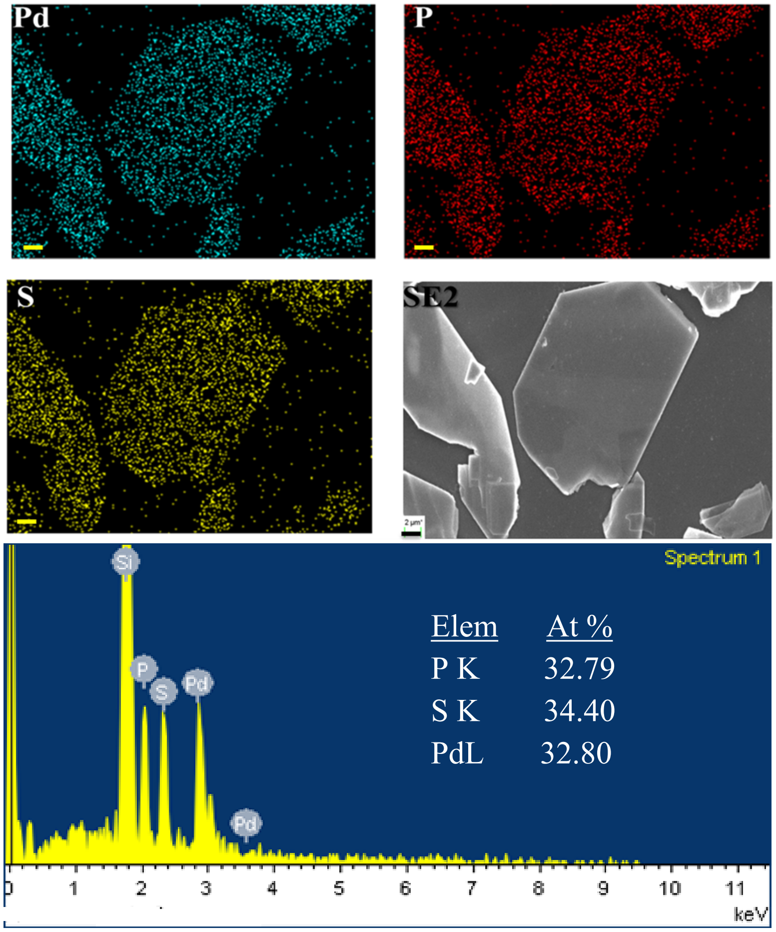

Elem	At %
P K	32.79
S K	34.40
PdL	32.80

Figure S1.a) Schematic representation of PdPS crystal (adopted and re-drwan from reference 1 given at the end) and neighbouring environment of PdPS crystal (adopted and redrawn from reference 2 given at the end). b) Elemental mapping (scale bar is 2 µm) and EDS analysis of bulk PdPS. The elemental mapping of Pd, P and S are shown. They are present with equal atomic ratio.

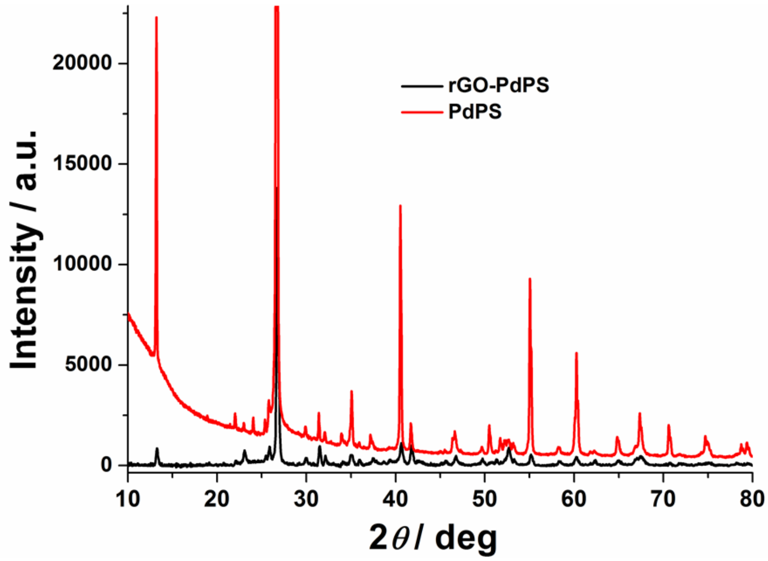

Figure S2. X-ray diffraction patterns for PdPS crystal and its composite with reduced graphene oxide, prepared by hydrothermal method.

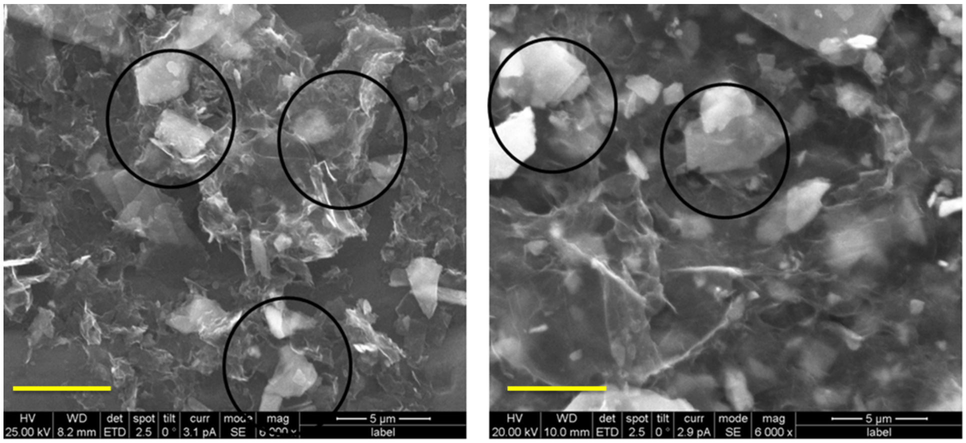

Figure S3. SEM micrographs of rGO-PdPS composite. PdPS crystals (marked in circle) are distributed over reduced graphene oxide sheets. (scale bar : 5 µm)

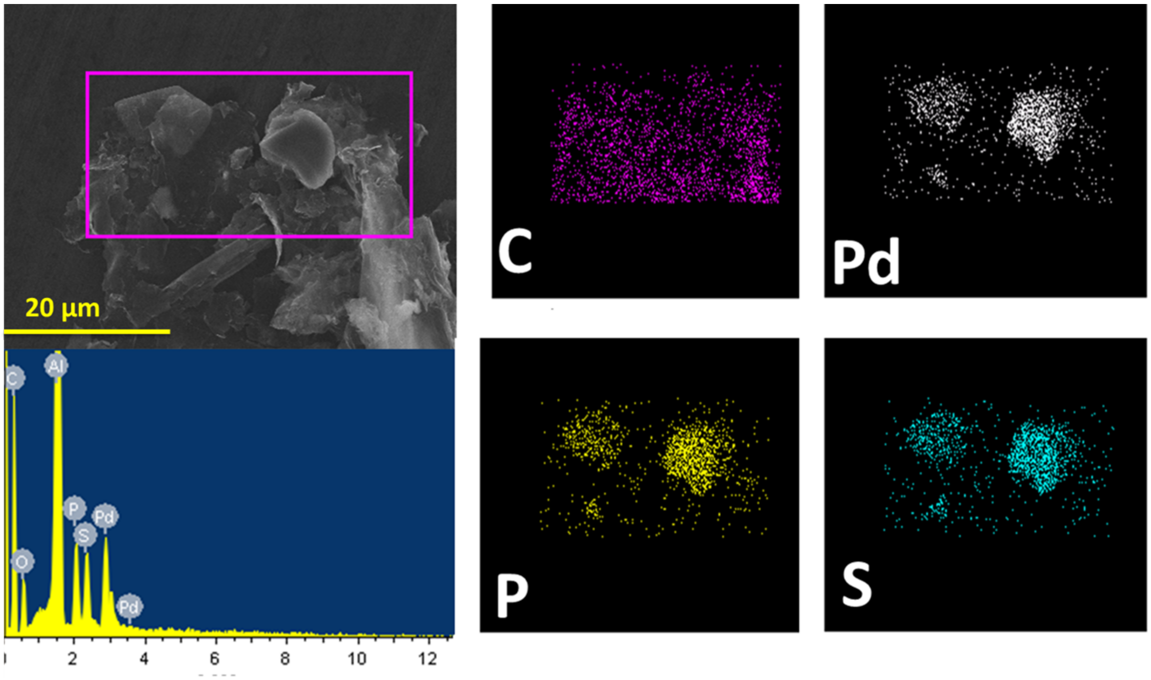

Figure S4. EDS analysis and elemental mapping of rGO-PdPS composite showing the presence of elements Pd, P, and S along with C. The box represents the focused area considered for mapping.

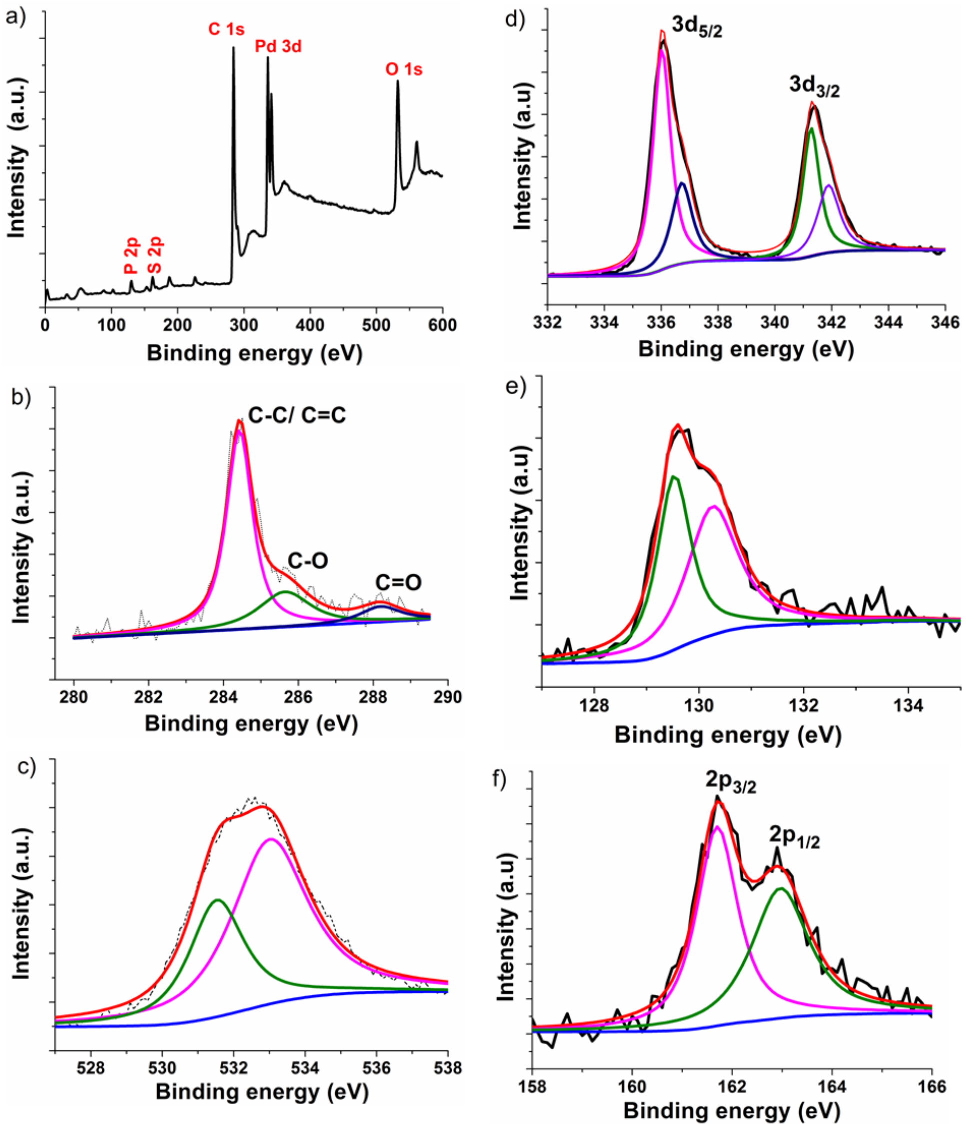

Figure S5. XPS survey spectra and high-resolution XPS spectra of PdPS. (a) Survey spectrum, (b) C1s, (c) O1s, (d) Pd 3d, (e) P 2p and (f) S 2p regions in the rGO-PdPS composite.

The high resolution C1s peak in rGO-PdPS composite is deconvoluted into 3 peaks. The peaks for C-C or C-H appear at binding energy values of 284.4 eV while C-O and C=O are present at 285.6 eV and 288.2 eV respectively, indicating the reduction of oxygen containing functional groups of graphene oxide during hydrothermal treatment. The changes observed on Pd3d, P2p and S2p levels are given below.

Table S1: Binding energies of corresponding core levels of PdPS and rGO-PdPS and the observed shift values.

XPS core level	Binding energy PdPS (eV)	Binding energy rGO-PdPS (eV)	Observed shift (eV)
Pd $3d_{5/2}$	335.7 336.2	335.9 336.7	0.3±0.1
Pd $3d_{3/2}$	340.9 341.5	341.3 341.9	
P	128.6 129.2	129.5 130.2	0.9±0.1
S $2p_{3/2}$	160.8	161.6	0.8
S $2p_{1/2}$	162.1	162.9	

Between bulk PdPS and rGO-PdPS, the shift observed in the case of Pd is (0.3±0.1) eV while in the case of S-2p levels, it is 0.8 eV and for 'P', the shift observed is 0.9 and 1.0 eV. Though small in magnitude, the shifts are clearly higher in the case of 'P' and 'S' as opposed to that of 'Pd'. It is likely that there is an interaction between rGO and P / S thus resulting in a shift of binding energy values. Carbon when doped with 'P'results in a positive shift of P level to 131 eV (P-C bond; D-S Yang et al., Carbon, 2014, 67, 736) while the P level for P-O in phosphorous doped graphene is observed at 133 eV (RSC Adv. 2013, 3, 9978). In the present study, the P level is shifted to 130.2 from 129.2. Though the shift is not to the same extent as that of the reported values in the references cited above, it is possible that there is an interaction between rGO and P / S thus leading to high HER activity.

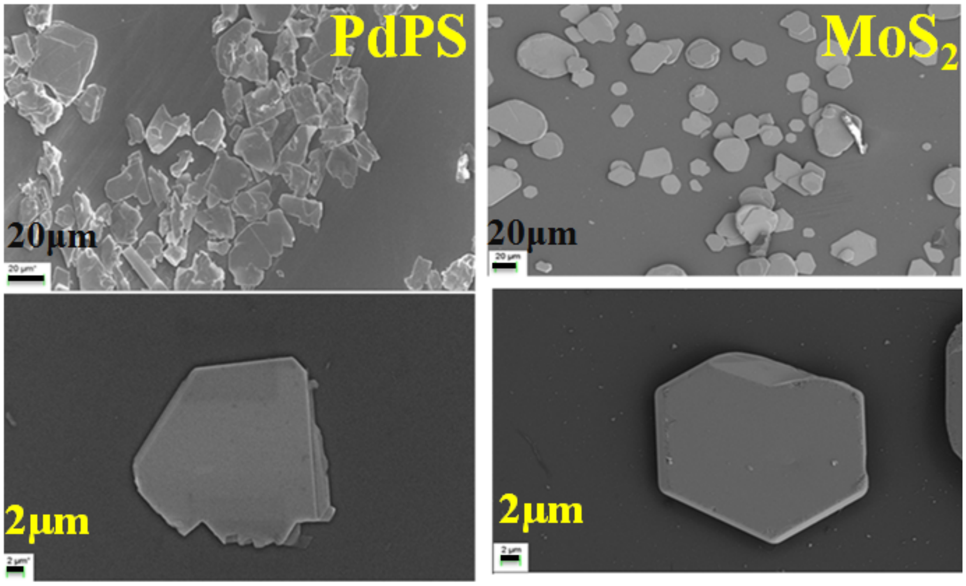

Figure S6. Low and high magnification SEM micrographs of as-synthesized, bulk PdPS (left) and bulk MoS_2 (right). The average size of the crystals is 20 ± 5μm.

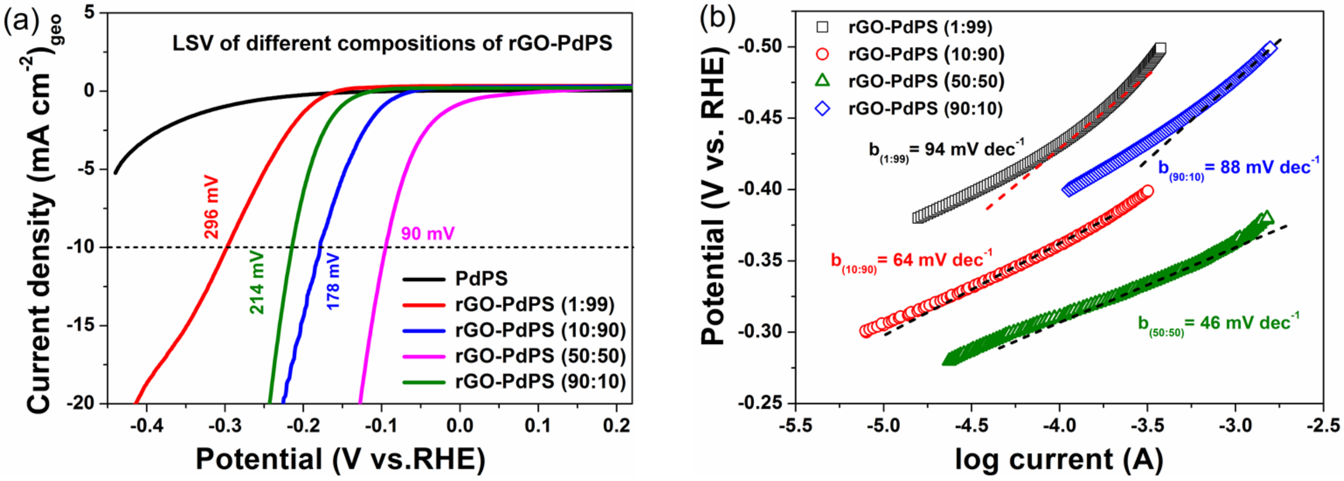

Figure S7. a) Linear sweep voltammograms of different mass ratio (1:99, 10:90, 50:50, 90:10) of rGO-PdPS composite in 0.5 M H_2SO_4 solution; scan rate 1 mV s^{-1}. The mass loading was maintained same in all the compositions. The dotted line shows the different overpotentials (η) need for different compositions to achieve 10 mA cm^{-2} cathodic current density. b) Tafel slopes for different mass ratio of rGO-PdPS in 0.5 M H_2SO_4 solution at a scan rate of 1 mVs^{-1}.

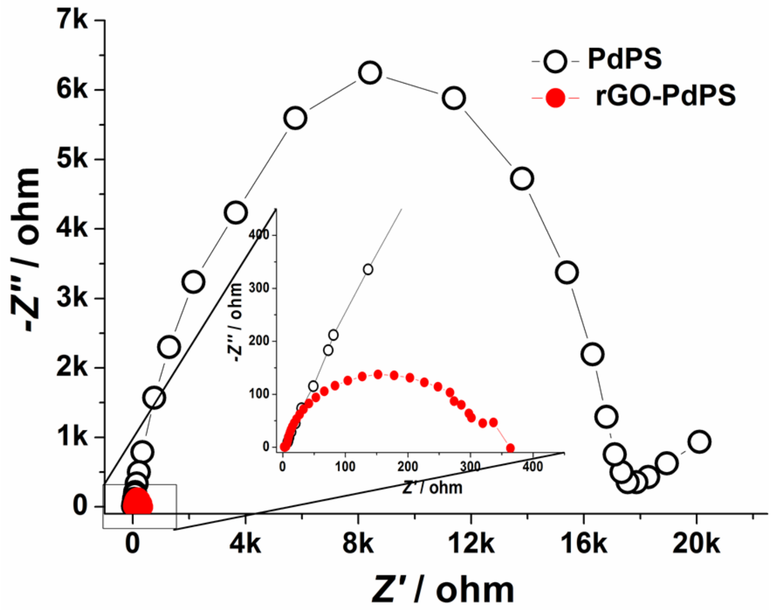

Figure S8. Nyquist plot of PdPS and rGO-PdPS. The DC bias used for the impedance studies is -0.04 V vs. RHE with 5 mV ac amplitude. The frequency range used for the studies is from 100 kHz to 10 mHz. The high frequency data is zoomed and represnted as inset.

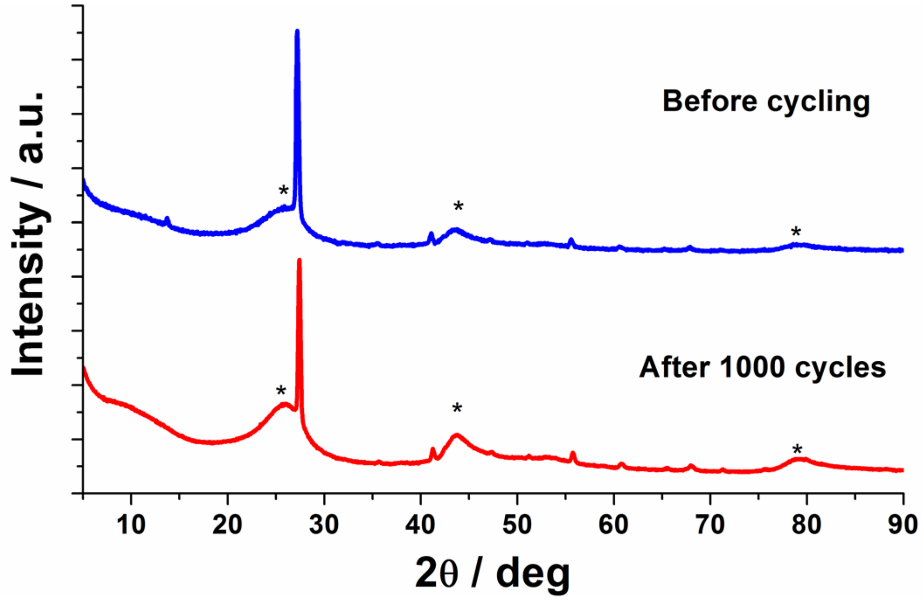

Figure S9. X-Ray diffraction patterns of rGO-PdPS composite on GC electrode surface before and after 1000 cycles. The peaks with * denote the contribution by the GC electrode.

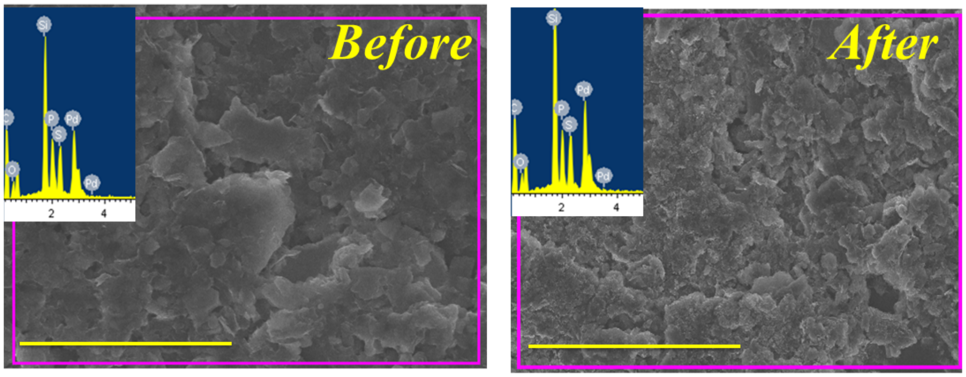

Elements	Before Cycling (Atomic %)	After Cycling (Atomic %)
C	63.58	64.55
O	16.21	15.21
Pd	3.72	4.01
P	3.46	3.37
S	3.30	3.10

Figure S10. SEM micrographs (scale bar: 100 µm) of rGO-PdPS on GC surface before and after 1000 cycles in 0.5 M H_2SO_4 solution. The atomic % of the elements based on EDS data (before and after cycling) are tabulated above.

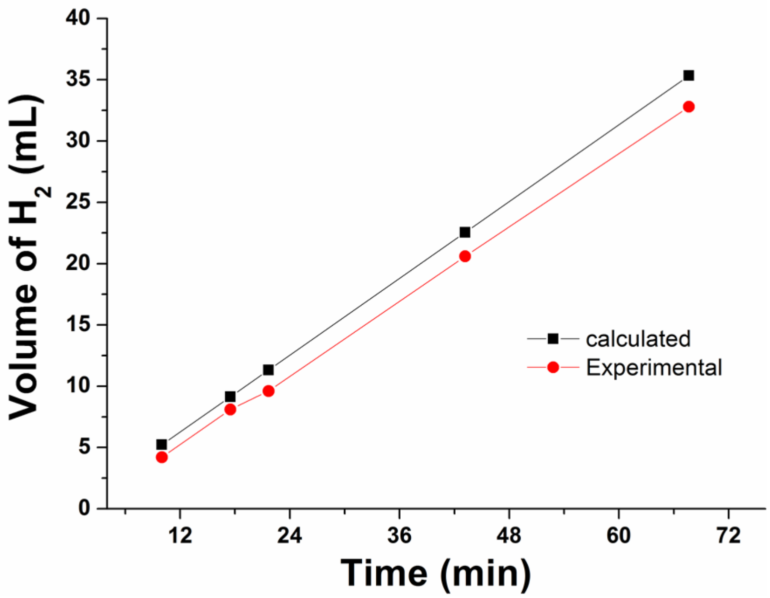

Figure S11. Volume of H_2 gas measured with time during galvanostatic electrolysis (Constant current of - 75 mA t is used and the electrode area is 0.45cm^2). The calculated values are based on Faraday's law.

Galvanostatic electrolysis

HER Electrolysis experiments are performed in a divided H- shaped cell. The counter electrode was separated from the solution through a porous glass frit. The rGO-PdPS modified GC (geometric area: 0.45 cm^2) electrode and SCE are kept in one part of the H-cell. The cell is air-tight and and a silicone tube is inserted inside the empty space of the cell while other part of the tube is kept inside the burette. In the inversion burette method, water filled burette is kept inversely in a water bath. Prior to the experiment, the solution is purged with N_2 gas for several tens of miutes and the electrolysis is carried out for an hour.

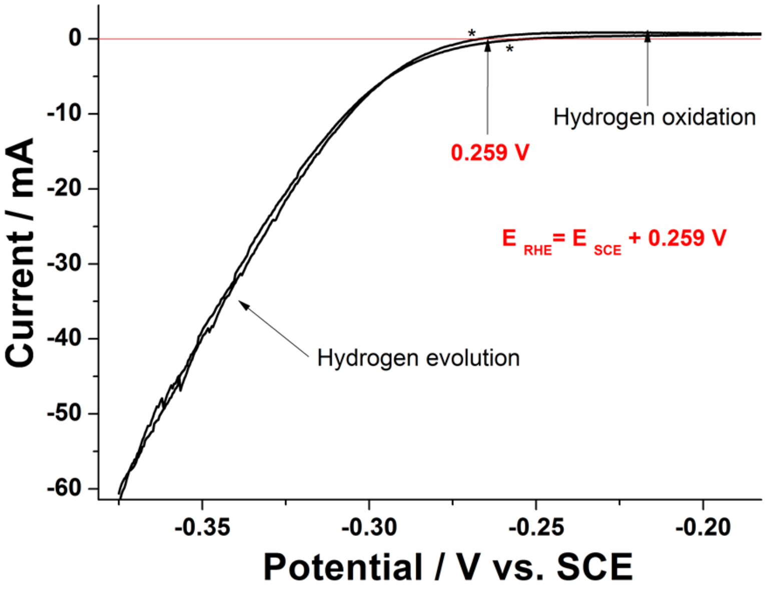

Figure S12. RHE calibration of SCE under hydrogen saturated 0.5 M H_2SO_4. The voltammograms is carried out at a scan rate of 1 mVs^{-1}.

RHE calibration:

Saturated calomel electrode (SCE) is used as the reference electrode for all measurements. The reference electrode is calibrated with respect to RHE[3] and the calibration is performed in high purity hydrogen saturated 0.5 M H_2SO_4 solution with Pt foil as the working and counter electrodes. Cyclic voltammetry (CV) is carried out at a scan rate of 1 mVs^{-1}. Average of the two potentials at which the currents crossed zero is identified as the thermodynamic potential for the hydrogen electrode reaction. In 0.5 M H_2SO_4 solution, E(RHE) = E(SCE) + 0.259 V.

Table S2: Electrochemical parameters for HER reported on various catalysts. References are from the main manuscript.

Catalyst	Current Density	Overpotential	Electrolyte	Reference
rGO-PdPS (2.5 mg/cm^2)	10 mA/cm^2	90 mV	0.5 M H_2SO_4	This work
MoS_2/rGO (0.28 mg/cm^2)	10 mA/cm^2	150 mV	0.5 M H_2SO_4	16a
Bulk Mo_2C	20 mA/cm^2	~240 mV	0.5 M H_2SO_4	9
Mo_2C/ CNT (2 mg/cm^2)	10 mA/cm^2	~150 mV	0.1 M $HClO_4$	9
Bulk MoB	20 mA/cm^2	~240 mV	0.5 M H_2SO_4	10
Ni-Mo-N nanosheets (0.25 mg/cm^2)	3.5 mA/cm^2	~200 mV	0.1 M $HClO_4$	36
Ni-Mo nanopowder (3 mg/cm^2)	10 mA/cm^2	80 mV	0.5 M H_2SO_4	35
Ni_2P nanostructures (1mg/cm^2)	20 mA/cm^2	130 mV	0.5 M H_2SO_4	8a
WS_2 nano sheets (0.285 mg/cm^2)	9.66 mA/cm^2	150 mV	0.5 M H_2SO_4	6b

Mo_1Soy/rGO	10 mA/cm^2	177 mV	0.1 M $HClO_4$	15
2H-MoS_2 nanosheet 1T-MoS_2 Nanosheet	10 mA/cm^2 10 mA/cm^2	320 mV 187 mV	0.5 M H_2SO_4	28a
MoS_2/mesoporous graphene (0.21 mg/cm^2)	100 mA/cm^2	200 mV	0.5 M H_2SO_4	16b
Oxygenated MoS_2 nanosheet (0.285 mg/cm^2)	126.5 mA/cm^2	300 mV	0.5 M H_2SO_4	28b
Defect rich MoS_2 (0.285 mg/cm^2)	70. 5 mA/cm^2	300 mV	0.5 M H_2SO_4	28c

References:

1. A. J. Foecker and W. Jeitschko, Journal of Solid State Chemistry; 2001, **162**, 69.
2. W. Jeitschko, Acta Cryst. 1974. **B30**, 2565.
3. M.-R. Gao, Z.-Y. Lin, T.-T. Zhuang, J. Jiang, Y.-F. Xu, Y.-R. Zheng, S.-H. Yu, J. Mat. Chem. 2012, **22**, 13662-13668